Ultrafast solvation response in room temperature ionic liquids: Possible origin and importance of the collective and the nearest neighbour solvent modes

Snehasis Daschakraborty and Ranjit Biswas

Citation: J. Chem. Phys. **137**, 114501 (2012); doi: 10.1063/1.4752425
View online: http://dx.doi.org/10.1063/1.4752425
View Table of Contents: http://jcp.aip.org/resource/1/JCPSA6/v137/i11
Published by the American Institute of Physics.

Ultrafast solvation response in room temperature ionic liquids: Possible origin and importance of the collective and the nearest neighbour solvent modes

Snehasis Daschakraborty and Ranjit Biswas[a)]
Chemical, Biological and Macromolecular Sciences, S. N. Bose National Centre for Basic Sciences, JD Block, Sector III, Salt Lake, Kolkata 700098, India

(Received 28 May 2012; accepted 30 August 2012; published online 17 September 2012)

Recent three-pulse photon echo peak shift (3PEPS) measurements [M. Muramatsu, Y. Nagasawa, and H. Miyasaka, J. Phys. Chem. A **115**, 3886 (2011)] with several room temperature ionic liquids (RTILs) have revealed multi-exponential dynamics with ultrafast solvation timescale in the range, $20 < \tau_1/fs < 250$, for both imidazolium and phosphonium RTILs. This is striking for two reasons: (i) the timescale is much faster than those reported by the dynamic Stokes shift (DSS) experiments [S. Arzhantsev, H. Jin, G. A. Baker, and M. Maroncelli, J. Phys. Chem. B **111**, 4978 (2007)] and (ii) sub-hundered femtosecond solvation response in phosphonium ionic liquids is reported for the first time. Here, we present a mode coupling theory based calculation where such ultrafast solvation in 3PEPS measurements has been visualized to originate from the nearest neighbour solute-solvent interaction. Consideration of Lennard-Jones interaction for the nearest neighbour solute-solvent non-dipolar interaction leads to biphasic dynamics with a predicted ultrafast time constant in the ∼100–250 fs range, followed by a slower one similar to that reported by the 3PEPS measurements. In addition, the calculated fast time constants and amplitudes are found to be in general agreement with those from computer simulations. Different microscopic mechanisms for ultrafast solvation response measured by the 3PEPS and DSS experiments have been proposed and relative contributions of the collective and nearest neighbour solvent modes investigated. Relation between the single particle rotation and ultrafast polar solvation in these RTILs has been explored. Our analyses suggest 3PEPS and DSS experiments are probably sensitive to different components of the total solvation energy relaxation of a laser-excited dye in a given ionic liquid. Several predictions have also been made, which may be re-examined via suitable experiments. © *2012 American Institute of Physics*. [http://dx.doi.org/10.1063/1.4752425]

I. INTRODUCTION

Recent three pulse photon echo peak shift (3PEPS) measurements[1] using an organic dye, oxazine 4 (Ox4), in a phosphonium and several imidazolium ionic liquids (ILs) at room temperature have revealed multi-exponential solvation response function possessing an ultrafast component (∼10%–25%) with time constant (τ_1) in 20–220 fs range, followed by a slower component with time constant (τ_2) spreading over nearly a picosecond to a few picoseconds. In some imidazolium ILs, another much slower component with time constant in the range, $20 < \tau_3/ps < 65$, has also been reported. These results are quite striking because of the following reasons: (i) the ultrafast timescale reported by 3PEPS measurements are much faster than those observed in the dynamic Stokes shift (DSS) experiments where complete detection of the dynamics has been performed[2] and (ii) these measurements report, for the first time, sub-hundred femtosecond solvation timescale even for a phosphonium IL which, in earlier complete DSS measurements,[3] showed stretched exponential response with only one relaxation time constant of ∼2 ns. Table I summarizes the solvation time constants reported by the 3PEPS and DSS measurements for some of these room temperature ionic liquids (RTILs), which brings out clearly the differences stated above. Understanding the molecular origin behind such an observation constitutes the central theme of the present paper where attempts have been made to ascertain mechanisms for ultrafast solvation revealed by these two different experimental methods.

The above theme then necessitates the following, somewhat detail, discussion of the results obtained by the 3PEPS and DSS measurements. These 3PEPS measurements have used oxazine 4 (Ox4) as a probe molecule, which shows steady state Stokes shift values in 200–500 cm^{-1} range for these RTILs. Such a small shift is in fact a characteristic[4] for Ox4 and can probably be attributed to its weakly polar ground (S_0) and even less polar excited (S_1) states.[5] Moreover, it has been found that solvent dependence of ultrafast solvation dynamics of Ox4 in conventional molecular liquids cannot be described by dielectric relaxation based theories.[6–10] DSS measurements, on the other hand, have employed dipolar chromophores such as coumarin 153 (C153),[3,11–14] 4-aminophthalimide (4AP),[15] and trans-4-dimethylamino-4′-cyanostilbene (DCS),[2] which undergo large dipole moment changes upon excitation. As a result, Stokes shift values for

a)Author to whom correspondence should be addressed. Electronic mail: ranjit@bose.res.in.

TABLE I. Comparison of solvation time constants reported by 3PEPS and DSS measurements.

Ionic liquid	Route	τ_1 (fs)	τ_2 (ps)	τ_3 (ps)
[Bmim][BF_4]	3PEPS	110	1.1	21
	DSS	320		130
[Bmim][PF_6]	3PEPS	150	2.2	64
	DSS	330		140
[Bmim][TFSI]	3PEPS	26	0.54	
	DSS	740		78
[Phos][Cl]	3PEPS	24	0.53	
	DSS	×	×	1860

these probes in phosphonium and imidazolium ionic liquids have been found to be approximately an order of magnitude larger than those with Ox4, and dynamic response explainable by a semi-molecular theory[16–21] that uses experimental dielectric relaxation data[22–25] as inputs. These contrasting results along with those discussed in the above paragraph then give rise to the following question: do 3PEPS and DSS experiments probe different aspects of solute-solvent interaction while measuring the solvation energy relaxation in these RTILs? The question becomes even more pertinent when one recalls that earlier 3PEPS studies of solvation dynamics in ambient alcohols (albeit with different solutes)[26] produced much faster timescales than those reported by DSS[27] and transient absorption (TA)[28] measurements, and subsequently, a possible resolution to the debate in terms of solute-solvent nearest neighbour non-polar type interaction was provided.[29] Since peak shift in 3PEPS measurements is related to the line-broadening function[30,31] which is determined by the total solvation energy correlation function and Stokes shift,[26,29] it is quite natural that both polar and non-polar solute-solvent interaction energies contribute to the observed dynamics. Moreover, experimental studies of non-dipolar solvation dynamics in conventional molecular solvents[32–36] have revealed Stokes shift ranging from a few hundred to several hundred cm^{-1}, which is much smaller than those observed in the cases of polar solvation. All these indicate a possible role for non-dipolar solvation dynamics to the timescales measured by the 3PEPS experiments. One therefore needs to investigate the timescales that may arise from interactions, which possess spatial dependence shorter-ranged than the dipole-dipole ($u_{id} \propto r^{-3}$) interaction.

What we do next is as follows. Relatively smaller Stokes shift for Ox4 in seven different ILs,[1] namely, [Bmim][Cl], [Bmim][BF_4], [Bmim][PF_6], [Bmim][TFSI], [Emim][TFSI], [Hmim][TFSI], and [Phos][Cl] motivates us to assume solute-IL interaction is primarily non-dipolar in nature. The chemical structures of these RTILs, and probe molecules, Ox4 and C153, are shown in Fig. 1. For simplicity, we approximate the non-dipolar interaction as purely a non-polar interaction given by the conventional Lennard-Jones (LJ) 6–12 interaction.[36] The total dynamics is predicted in terms of solute-solvent binary collision and collective structural relaxation through a mode-coupling approach.[37–39] Evidently, the binary collision part describes the initial ultrafast response where solvent distribution around a solute at extremely short time is approximated by the equilibrium radial distribution function.[36] This amounts to stating that the solute is trapped inside a solvent cage at short time where collision against the solvent cage carries out the initial phase of the solvation energy relaxation. The structural relaxation part, governed by the solvent density fluctuations (and hence connected to the medium viscosity), then takes over and accounts for the slower component of the total solvation energy relaxation.[40] In other words, a clear separation between the collisional and density fluctuation timescales are assumed *a priori*. The timescales associated with the nearest neighbour ($k\sigma \rightarrow 2\pi$) and collective ($k\sigma \rightarrow 0$) solvent density modes for the structural relaxation part are then explored. Subsequently, the origin for the ultrafast polar solvation response is investigated by testing the relation between solvent rotation (here imidazolium ILs) and polar solvation energy relaxation. Experimental dielectric relaxation data at the microwave frequency range have been used for such an investigation in order to either minimize or avoid contributions from the solvent translation-rotation coupling (conductivity contribution), which appears at the terahertz (THz) regime.[41–43] Finally, a comparative study between the calculated results and those obtained from 3PEPS, DSS, and computer simulations[44–57] is presented, which suggests that these different experimental methods probe different aspects of the solute-IL interaction.

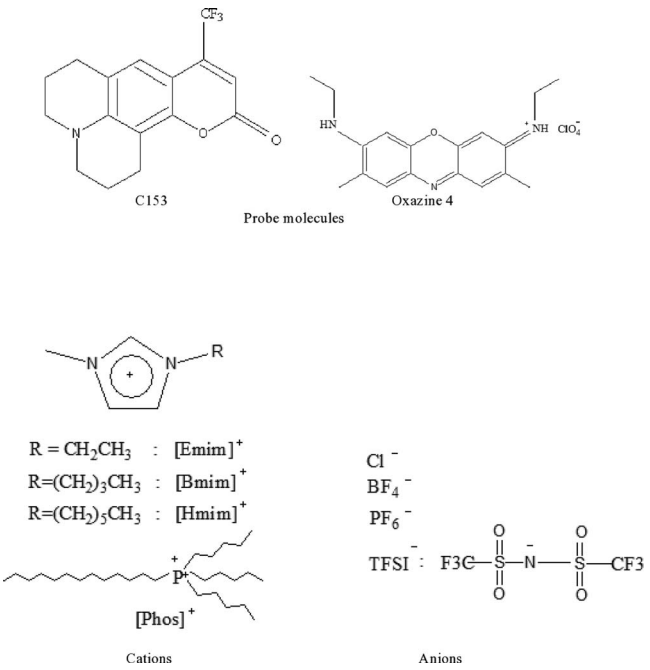

FIG. 1. Schematic representations of the solute probes and the ions constituting the ionic liquids considered in the present work.

II. THEORY AND CALCULATION DETAILS

The normalized solvation energy-energy time correlation function, $S_{NP}(t)$, for the solute interacting with the solvent molecules via nonpolar interaction can be written as[39]

$$S_{NP}(t) = \frac{C_{EE}^{NP}(t)}{C_{EE}^{NP}(t=0)}, \quad (1)$$

where $C_{EE}^{NP}(t)$ is the un-normalized nonpolar solvation energy time correlation function. Following the prescription described earlier,[39] $C_{EE}^{NP}(t)$ can be given by the following expression:

$$C_{EE}^{NP}(t) = C_{EE}^{B}(t=0)\exp\left[-\left(t/\tau_E^B\right)^2\right] + C_{\rho\rho}(t), \tag{2}$$

where τ_E^B is the relaxation time of the binary part of the energy-energy correlation function and is given by[39]

$$\tau_E^B = \sqrt{\frac{-2C_{EE}^B(t=0)}{\ddot{C}_{EE}^B(t=0)}}, \tag{3}$$

where $\ddot{C}_{EE}^B(t) = \frac{d^2C_{EE}^B(t)}{dt^2}$. At extremely short times, this binary part is determined by the solute-solvent interaction potential ($v_{12}(r)$) where the solvent distribution around the solute can be approximated by the solute-solvent radial distribution function, $g_{12}(r)$, weighted by the solvent density (ρ)[39,58]

$$C_{EE}^B(t=0) = 4\pi\rho\int_0^\infty dr\, r^2[v_{12}(r)]^2 g_{12}(r), \tag{4}$$

and

$$\ddot{C}_{EE}^B(t=0) = \frac{4\pi\rho}{m^*}\int_0^\infty dr\, r^2[v_{12}(r)]^2\nabla_r g_{12}(r)\nabla_r v_{12}(r), \tag{5}$$

where m^* denote the reduced mass of the solute-solvent composite system. Note in the above expressions, the following equality has been used: $G_{12}(r,\, t=0) = g_{12}(r)$, where $G_{12}(r,\, t)$ represent the distinct part of the van Hove correlation function.[36]

The slowly varying, density fluctuation contribution, $C_{\rho\rho}(t)$, is approximated as[40]

$$C_{\rho\rho}(t) = \frac{(k_BT)^2\rho}{6\pi^2}\int_0^\infty dk\, k^2 c_{12}^2(k) S(k,t), \tag{6}$$

where $c_{12}(k)$ being the wave-number, (k) dependent solute-solvent direct correlation function, and k_BT the Boltzmann constant times the absolute temperature. $c_{12}(k)$ has been obtained by using the Weeks-Chandler-Andersen (WCA) scheme.[59] Subsequently, the dynamic solvent structure factor, $S(k,\, t)$, has been calculated by using the relation[37,60]

$$S(k,t) = L^{-1}\left[\frac{S(k)}{z + \langle\omega_k^2\rangle\left[z + \Delta_k\left(z + \tau_k^{-1}\right)^{-1}\right]^{-1}}\right], \tag{7}$$

where L^{-1} denotes the Laplace inversion operator, which is performed numerically by using the Stehfest algorithm.[61] z is the frequency. The static solvent structure factor, $S(k)$, is obtained from the solutions of the Percus-Yevick (PY) equation for binary mixture of hard spheres.[62] $\langle\omega_k^2\rangle = [k_BTk^2/mS(k)]$, m being the mass of a solvent molecule, $\tau_k^{-1} = 2\sqrt{(\Delta_k/\pi)}$, and $\Delta_k = \omega_l^2(k) - \langle\omega_k^2\rangle$. $\omega_l^2(k)$ is the second moment of the longitudinal current correlation function expressed as[37]

$$\omega_l^2(k) = 3m^{-1}k^2k_BT + \omega_0^2 + \gamma_d^l(k), \tag{8}$$

where the longitudinal component of the vertex function, $\gamma_d^l(k)$, and the Einstein frequency of the solvent, ω_0, can be calculated from the solvent-solvent interaction potential, $v(r)$, and the radial distribution factor, $g(r)$, from the following expressions:[37–39]

$$\gamma_d^l(q) = -m^{-1}\rho\int d\boldsymbol{r}\, \exp(-i\boldsymbol{k}\cdot\boldsymbol{r})g(r)\frac{\delta^2}{\delta z^2}(v(r)), \tag{9}$$

and

$$\omega_0^2 = 3m^{-1}\rho\int d\boldsymbol{r}\, g(r)\nabla^2 v(r). \tag{10}$$

It is evident therefore that once the solute-solvent and solvent-solvent interaction potentials (non-polar) are specified, the solvation response function using Eq. (1) can be easily evaluated. As already mentioned, we have used the traditional 6–12 LJ potential to represent the solute-solvent and solvent-solvent interactions.

The solute-solvent radial distribution function, $g_{12}(r)$, required in Eqs. (4) and (5), is calculated from partial structure factor.[63,64] The partial structure factors ($S_{ij}(k)$) are the (i, j) elements of the structure factor matrix (S(k)). For binary mixtures, S(k) is written as follows:[63,64]

$$\mathrm{S}(k) = \begin{pmatrix} S_{11} & S_{12} \\ S_{21} & S_{22} \end{pmatrix}. \tag{11}$$

Similarly, the partial direct correlation function ($c_{ij}(k)$) are the (i, j) elements of the direct correlation function matrix (c(k)). S(k) and c(k) are connected via the following relation:

$$\mathrm{S}(k) = [1 - \rho\mathrm{c}(k)]^{-1}, \tag{12}$$

where $\boldsymbol{1}$ denotes the identity matrix.

Hence, the partial structure factors can be written as

$$S_{11}(k) = \left\{1 - \rho_1 c_{11}(k) - \frac{\rho_1\rho_2 c_{12}^2(k)}{1 - \rho_{22}c_{22}(k)}\right\}^{-1}, \tag{13}$$

$$S_{22}(k) = \left\{1 - \rho_2 c_{22}(k) - \frac{\rho_1\rho_2 c_{12}^2(k)}{1 - \rho_{11}c_{11}(k)}\right\}^{-1}, \tag{14}$$

$$S_{12}(k) = (\rho_1\rho_2)^{1/2}c_{12}(k)\{[1 - \rho_1 c_{11}(k)][1 - \rho_2 c_{22}(k)] - \rho_1\rho_2 c_{12}^2(k)\}^{-1}. \tag{15}$$

We have calculated the direct correlation functions, $c_{ij}(k)$, by using the method mentioned earlier[62] via the WCA scheme.

If one considers the ion-ion interaction in addition to the LJ potential for solvent-solvent interaction, solvent-solvent direct correlation functions can be approximated by the pair correlation function ($h_{\alpha\beta}(k)$)[65,66]

$$h_{\alpha\beta}(k) = -\frac{4\pi\, q_\alpha q_\beta}{\varepsilon_0 k_B T(1+\kappa\sigma)}\frac{\kappa^2}{\kappa_D^2(k^2+\kappa^2)} \times\left[\cos k\sigma + \frac{\kappa}{k}\sin k\sigma\right], \tag{16}$$

where σ is the ionic diameter, and κ is related to the Debye screening parameter κ_D by

$$\kappa = \frac{\kappa_D}{[1 - (\kappa_D\sigma)^2/2 + (\kappa_D\sigma)^3/6]^{1/2}}, \tag{17}$$

TABLE II. Comparison between the solvation time constants obtained from the calculated non-polar solvation energy relaxation and those from 3PEPS measurements.

Ionic liquid	Route	a_1	τ_1 (fs)	a_2	τ_2 (ps)	a_3	τ_3 (ps)	$\langle\tau\rangle$ (ps)
[Bmim][Cl]	3PEPS		26		0.54			
	Calculation	0.93	99	0.07	1.99			0.23
[Bmim][BF_4]	3PEPS		110		1.10		21	
	Calculation	0.92	232	0.08	3.01			0.45
[Bmim][PF_6]	3PEPS		150		2.2		64	
	Calculation	0.89	225	0.11	2.76			0.52
[Bmim][TFSI]	3PEPS		210		3.10		52	
	Calculation	0.87	148	0.13	1.62			0.34
[Emim][TFSI]	3PEPS		220		2.70		20	
	Calculation	0.89	183	0.11	2.12			0.40
[Hmim][TFSI]	3PEPS		200		3.30		37	
	Calculation	0.89	210	0.11	2.44			0.46
[Phos][Cl]	3PEPS		24		0.53			
	Calculation			0.89	0.48	0.11	5.75	0.71

with

$$\kappa_D = \left(\frac{4\pi}{\varepsilon_0 k_B T}\sum_\alpha \rho_\alpha q_\alpha^2\right)^{1/2}, \tag{18}$$

where ε_0 is the static dielectric constant of the medium, ρ_α the density of and q_α the charge on the αth species. Note the Debye screening length, κ_D^{-1}, for these RTILs is even less than 1Å and thus unrealistic as a screening length for these molecular systems.[67,68] In addition, Eq. (16) describes static correlations in ionic solutions at the long wavelength (that is, $k\sigma \rightarrow 0$) limit. As a result, correlations calculated using Eq. (16) is likely to be inaccurate for dynamical events that are regulated by correlations at the molecular length scales. This may lead to improper predictions of RTIL dynamics.

III. NUMERICAL RESULTS AND DISCUSSIONS

A. Ultrafast solvation response measured by 3PEPS experiments: Possible origin

Calculated decays of the nonpolar solvation response function, $S_{NP}(t)$, are shown in Figure 2 for five representative RTILs, [Bmim][Cl], [Bmim][BF_4], [Bmim][PF_6], [Bmim][TFSI], and [Phos][Cl]. These calculations are done with solute-IL size ratio, $R = \sigma_{solute}/\sigma_{IL} = 1$, σ being the molecular diameter,[2,3,69] and at the respective RTIL densities.[70] Note that fixing the solute-IL size ratio at unity for these calculations may not be quite unphysical as Ox4 (size unavailable) is structurally very similar to C153 whose molecular diameter is known.[27] Data on size ratio provided in Table S1 (see supplementary material[71]) suggest that imidazolium ILs, particularly those with non-TFSI anions, possess a size ratio nearly unity against a solute similar to the size of C153. Other parameters necessary for calculations are provided in Table S2.[71] The calculated decays exhibit an anion dependence which has already been reported by the 3PEPS measurements.[1] A closer inspection of Fig. 2 also reveals an anion sequence in terms of non-polar solvation energy decay rate in imidazolium ILs ($Cl^- > BF_4^- > PF_6^-$), which is the same as observed in experiments.[1] However, the decay predicted for [Phos][Cl] is the slowest and thus completely different from the 3PEPS results. Calculated decays shown here are bimodal and nicely fit to a sum of Gaussian and exponential components having the following form: $S_{NP}^{fit}(t) = a_1 \exp(-(t/\tau_1)^2) + a_2 \exp(-t/\tau_2)$. Parameters obtained from such fits summarized in Table II indicate overwhelming dominance (~90%) of the Gaussian component with a time constant (τ_1) in ~100–250 fs range. The slow, exponential component with a time constant (τ_2) of 2–3 ps then carries out the remaining part of the $S_{NP}(t)$ decays in these RTILs. Time constants obtained from 3PEPS measurements are also shown in Table II, and a comparison reveals semi-quantitative agreement between the predicted and measured τ_1 and τ_2 except for [Phos][Cl]. Interestingly, the slowest time constant from 3PEPS measurements ($\tau_2 = 0.53$ ps) for [Phos][Cl] is quite close to τ_1 from theory but the predicted slower time constant (~6 ps) has not been detected in experiments with this RTIL. We have found that equally good description of the calculated decays could be obtained by fitting to a function consisting of a Gaussian and two exponentials producing a third but negligibly small component (~1%) with a time constant (τ_3) in 20–60 ps range (τ_1 and τ_2 remaining more

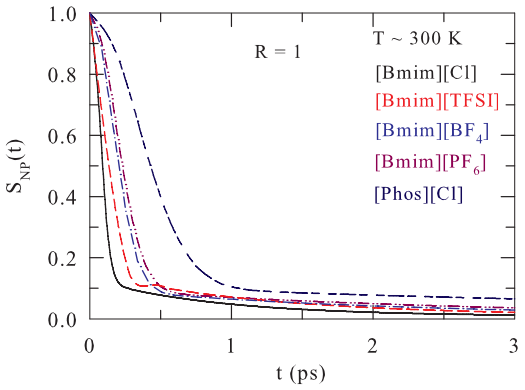

FIG. 2. Calculated decays of the nonpolar solvation response function in five different ionic liquids, [Bmim][Cl], [Bmim][TFSI], [Bmim][BF_4], [Bmim][PF_6], and [Phos][Cl] at ~300 K. The solute-solvent size-ratio has been considered to be unity for each of the cases. Note the curves are color coded.

or less unchanged). Although this third time constant is in the same range as found in 3PEPS measurements with some of the imidazolium ILs, the smallness of the associated amplitude does not confidently suggest its real presence in our calculated $S_{NP}(t)$.

The time constants and amplitudes obtained from fits to the $S_{NP}(t)$ decays bear some similarities with those from the simulated solvation response functions for many different ILs with a variety of solutes.[44–57] For example, a very recent simulation study of solvation dynamics in a model IL mimicking [Bmim][PF_6] at 350 K has reported, depending upon solute size and type of solute electronic perturbation, ultrafast Gaussian solvation response characterized by a time scale in ~200–400 fs range with ~30%–65% amplitude.[44] Simulation studies of solvation dynamics using model diatomic solutes in [Emim][PF_6] and [Emim][Cl] at 400 K have reported ultrafast Gaussian component (~30%–70%) with timescale in ~60–200 fs range.[46–48] This extremely fast timescale with an overwhelming amplitude (80%–90%) has also been found in the simulated solvation response for an ionic solute in another IL, [Dmim][PF_6] at 450 K.[52] Simulated solvation response for ions and dipole in [Dmim][Cl] at 425 K suggests an ultrafast Gaussian component with a time constant ~50–60 fs that accounts for nearly 80% of the total solvation energy relaxation.[53] Simulations of solvation dynamics using realistic solutes, such as betaine-30 and C153, in [Bmim][PF_6] at 300 K has revealed, on the other hand, a much less pronounced Gaussian component (~10%–30%) with a time constant of ~200 fs.[54,55] Subsequent simulations involving pyrrolidinium ILs and C153 at 400 K have reported the ultrafast component to be approximately 20% with time constant in ~200–300 fs range.[56,57]

In all the above simulations, the origin of the ultrafast solvation has been attributed to the nearest-neighbour solute-IL interaction. Interestingly, in the present calculations too, the ultrafast timescale emerges from the binary interaction of the solute with the molecules in the first solvation shell via the convolution of spatially dependent solute-solvent interaction with solute-solvent radial distribution function (see Eqs. (4) and (5)). According to these equations, it is the solute-solvent radial distribution function at contact (that is, $g_{12}(\sigma)$) that determines the ultrafast collisional timescale at a given liquid density and temperature. Therefore, this description for the ultrafast solvation is equivalent to what is already pointed out by simulations[44–56] and envisaged in Ref. 1 while explaining the 3PEPS results. However, there exists a subtle difference in the sense that the sub-picosecond response in almost all of these simulation studies[44,46–48,53–57] arises from the *electrostatic* solute-IL interaction, whereas the present calculations and the simulation works reported in Ref. 52 suggest non-polar solute-IL interaction as a source for such an initial ultrafast decay. This simulation study[52] monitored fluctuations in both electrostatic and LJ parts of the solute-IL interaction energy and found that equilibrium correlation functions constructed from these individual fluctuating components are characterized by damped oscillations with similar time periods (~350–500 fs). The striking resemblance between the calculated and simulated ultrafast timescales and the simulation finding that *the sub-picosecond response is due to changes in the nearest neighbour repulsion*[52] therefore indicate that the solute-IL nearest neighbour non-polar interaction can be one of the possible origins for the ultrafast solvation timescales revealed by the recent 3PEPS measurements[1] for several RTILs.

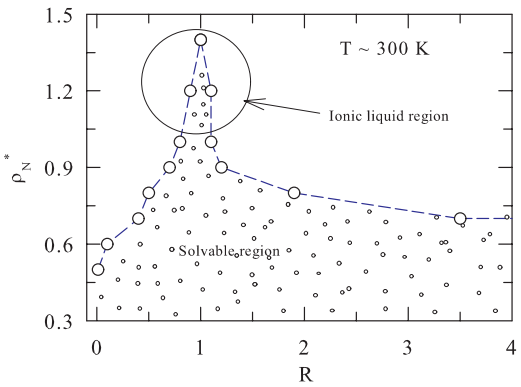

FIG. 3. Diagram showing the solvable region in the density-size ratio ($\rho_N^* - R$) space, where PY approximations for binary hard sphere mixtures provide stable solutions for the direct correlation functions. R denotes the ratio between the solute and IL sizes. The shaded area is the region where PY approximation works.

Before we elaborate further on the role of non-polar solute-solvent interaction in the ultrafast solvation energy relaxation in ILs, let us now explore the region in the density-size ratio ($\rho_N^* - R$) space where the PY approximations[62] for binary hard sphere mixtures provide stable solutions for the direct correlation functions. Here, ρ_N denotes the number density of a given IL and $\rho_N^* = \rho_N \sigma_{IL}^3$. Figure 3 demonstrates such a diagram where regions outside the boundary line are inaccessible to the present calculations due to the inability of the existing PY approximations to provide correct solutions for the direct correlation functions. It is evident from this figure that for liquids with densities as high as of these ILs, choice of a solute in the present calculations is rather narrow. For a solute 2–3 times larger than that of an IL molecule, one has to lower the IL density appreciably (from $\rho_N^* \sim 1.3$ to $\rho_N^* \sim 0.7$) in order for the present theory to work. This limitation notwithstanding, the current calculations can be employed to explore the solute size dependence of the ultrafast solvation response in ILs because a significant dependence on solute size has already been predicted for solvation via non-polar mechanism.[40] Such a solute size dependence for [Bmim][Cl] is presented in Fig. 4 where in the upper panel, the time constants (τ_1 and τ_2) obtained from fits to the $S_{NP}(t)$ decays calculated at $\rho_N^* = 0.7$ are shown as a function of R. Note the fast time constant, τ_1, decreases by about 20% for changing R from 1 to 3 while τ_2 (slower of these two) remains almost insensitive to the size ratio. The origin could be traced in the solute size dependence of the solute-solvent radial distribution function at contact, $g_{12}(\sigma)$, shown in the lower panel of Fig. 4, as a function of R. Here, also $g_{12}(\sigma)$ increases by ~20% for the same change in R. As $g_{12}(\sigma)$ regulates the solute-solvent interaction via structuring the first solvation shell, the dependence is more direct and hence the scaling is proportionate. This predicted solute size dependence of ultrafast solvation timescale in ILs may be tested against 3PEPS measurements since the latter can probe more accurately the nearest neighbour ($k\sigma \rightarrow 2\pi$) interactions.

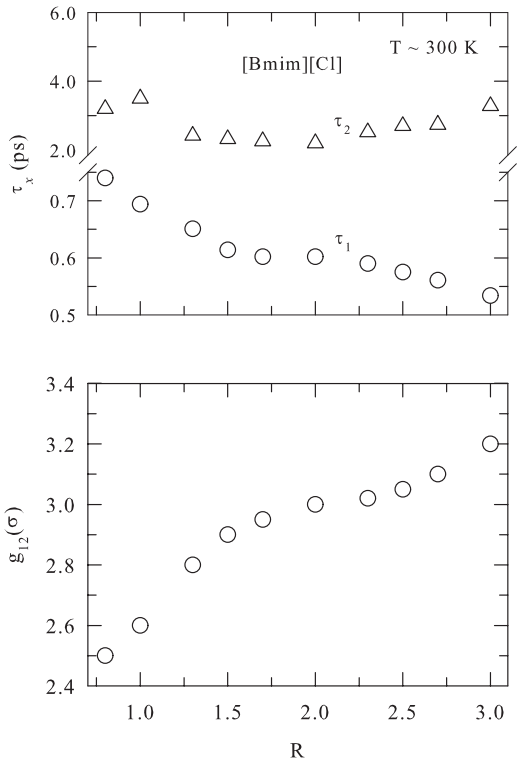

FIG. 4. Solute-IL size ratio (R) dependence of the non-polar solvation time constants (upper panel) and the value of the solute-IL radial distribution function at contact, $g_{12}(\sigma)$, for [Bmim][Cl] at ~300 K.

The dependence of ultrafast solvation time scale on $g_{12}(\sigma)$ brings into the picture the density dependence of solvation rate since $g_{12}(\sigma)$ is determined by the liquid density at a given temperature via the pressure equation.[36] Figure 5 depicts such a density dependence for $R = 1$ at T = 300 K where both τ_1 and τ_2 are shown as a function of reduced solvent density, ρ_N^*. Note in this figure that while τ_1 decreases steadily with density, τ_2 increases. This can be understood by considering the following physical picture. The increase in liquid density leads to more densely packed solvation structure around the probe solute. This is reflected in the density dependence of $g_{12}(\sigma)$, shown in the upper panel of Fig. S3 (see supplementary material[71]). This "more compact" solvation structure induces accelerated solvation energy relaxation via more effective solute-solvent interaction. This is binary in nature and the origin for τ_1 to become faster with ρ_N^*. The slower timescale (τ_2), on the other hand, becomes even slower with density because τ_2 is controlled by the structural relaxation (see Eq. (6)), which becomes slower as density increases. This is shown in the lower panel of Fig. S3 (see supplementary material[71]) where decays of the normalized wavenumber dependent solvent dynamic structure factor, $S(k\sigma, t)$, are compared for two different densities at two different wavenumbers. Note here that the decay corresponding to larger wavenumber is faster than that to smaller wavenumber, suggesting the slower timescale is associated with the collective density fluctuations. The average non-polar solvation time, shown also in Fig. 5, decreases with density because of the dominant amplitude (~90%) for the calculated ultrafast component. This prediction of solvent density induced fast component becoming faster and slow turning slower, which can be accessed via changing pressure at a fixed temperature, may be cross-examined via experiments and compared between ionic liquids and conventional molecular liquids. It is worth mentioning here that given the solute-solvent size ratio and density dependencies of the solvation timescales and also if one considers the possible change in solute-ion interactions due to change in conformational structure of larger ion such as TFSI,[72–74] the agreement between the calculated and measured timescales (Table II) may be termed as semi-quantitative. This is interesting as accurate modelling of shorter-ranged interactions in ionic liquids demands more complexity than the simple one presented here because of the heterogeneity inherent to these ILs[75–82] and variations in shape of the constituent ions.

Next we present in Fig. 6 the calculated solvation response functions for three different solute-IL size ratios after considering the ion-ion interaction in addition to the LJ interaction among IL molecules. This we may term as ionic LJ interaction, and used [Bmim][Cl] as the representative IL for the subsequent calculations. The term that is freshly calculated with this modified interaction is the density fluctuation contribution, $C_{\rho\rho}(t)$. The dissolved solute is, as before, a LJ particle and $\rho_N^* = 0.7$. Parameters describing the decays of the calculated response function (denoted as $S_{ILJ}(t)$) are also

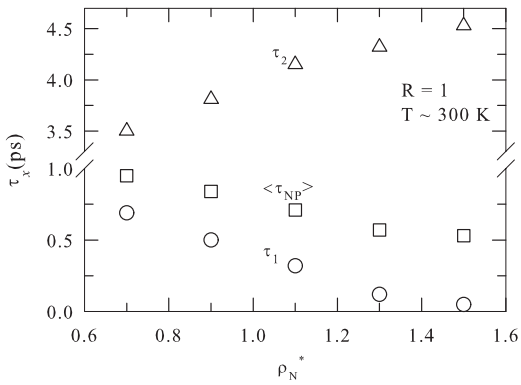

FIG. 5. Density dependence of nonpolar solvation time constants, τ_1, τ_2, and the nonpolar average solvation time, $\langle\tau_{NP}\rangle$, for $R = 1$ at ~300 K.

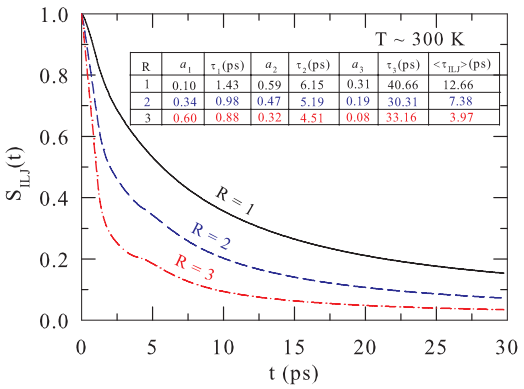

R	a_1	τ_1(ps)	a_2	τ_2(ps)	a_3	τ_3(ps)	$\langle\tau_{ILJ}\rangle$(ps)
1	0.10	1.43	0.59	6.15	0.31	40.66	12.66
2	0.34	0.98	0.47	5.19	0.19	30.31	7.38
3	0.60	0.88	0.32	4.51	0.08	33.16	3.97

FIG. 6. Normalized solvation response for [Bmim][Cl] at ~300 K for three different solute-IL size ratios after considering ion-ion interaction in addition to the nonpolar interaction while obtaining the IL-IL spatial correlations. Fit parameters are shown in the inset.

shown in the inset of this figure. It is evident from this figure that incorporation of the longer-ranged electrostatic interaction in the static ion structure factor ($S(k)$) via Eq. (16) leads to much slower relaxation of the solvation energy for a non-polar solute. As already discussed, this may be due to inaccurate description of the ion-ion correlations at the molecular length-scales by Eq. (16), which, in turn, has led to the incorrect prediction of the solvation energy relaxation. This is of course expected as Eq. (16) is based on continuum model description of systems possessing electrostatic interactions and describes static ion-ion correlations at the long wavelength (that is, $k\sigma \rightarrow 0$) limit. Even with this lacuna, the resultant calculations capture the solute size dependence in line with what has already been observed with pure solute-solvent and solvent-solvent non-polar interactions (shown in Fig. 4). This is because $g_{12}(r)$ in $C^B_{EE}(t)$ is still obtained from solute-IL non-polar interaction and dominates the total solvation energy relaxation via the initial ultrafast component.

B. Ultrafast solvation response measured by DSS experiments: Possible origin

We have already noticed in Table I that DSS measurements report ultrafast solvation timescale for imidazolium ILs much slower than that by the 3PEPS measurements. Inertial translation of the lighter ions (for these ILs the anions) has been believed to be the origin for the initial fast solvation response detected in DSS experiments.[2,83,84] However, this mechanism fails to explain why DSS measurements do not find any ultrafast component for [Phos][Cl] in which the anion is ~8 times lighter than the anion in [Bmim][TFSI], where DSS experiments report the presence of a fast component with time constant ~700 fs. Similar comparison also holds for the other two imidazolium ionic liquids where the anions are 2–4 times heavier than that in the [Phos][Cl]. Subsequently, a semi-molecular theory has successfully described the biphasic solvation energy relaxation in imidazolium ILs observed in DSS measurements by using the experimental dielectric relaxation data as input, and proposed the collective reorientational dynamics of the dipolar ions (for example, imidazolium cation in imidazolium ILs) as the source for the initial fast dynamics.[16–21] In addition, this theory describes the experimental Stokes shift dynamics in these ILs in terms of both solute-IL dipole-dipole and dipole-ion contributions, where the slow dynamics at long time has been ascribed to the relaxation of the ion dynamic structure factor via centre-of-mass ion motion. Since the above dielectric relaxation based theory has been discussed in detail elsewhere,[16–21] we will present here only the necessary equations for stressing the importance of the reorientational motion of the dipolar cations and the lengthscale involved in the orientational density fluctuation that produces the initial fast solvation response measured in these ILs. Later, we explore for an imidazolium IL, the validity of the approximate relationship between the single particle orientation and initial solvation response first proposed for explaining the short time dynamics in conventional, strongly polar liquids.[85,86]

The normalized solvation response function due to the fluctuating solute-IL dipole-dipole interaction energy (ΔE_{sd}) is as follows:[16–21]

$$S_{sd}(t) = \frac{\langle \Delta E_{sd}(t)\Delta E_{sd}(0)\rangle}{\langle \Delta E_{sd}(0)\Delta E_{sd}(0)\rangle}, \tag{19}$$

where the equilibrium dipole-dipole energy correlation function for a large and massive solute can be written as[16–21]

$$\langle \Delta E_{sd}(t)\Delta E_{sd}(0)\rangle = 2\rho_d^0 \left(\frac{k_B T}{2\pi}\right)^2 \int_0^\infty dk k^2 \Big[\big|c_{sd}^{10}(k)\big|^2 \times S_d^{10}(k,t) + 2\big|c_{sd}^{11}(k)\big|^2 S_d^{11}(k,t)\Big], \tag{20}$$

with ρ_d^0 being the equilibrium dipolar density, $c_{sd}^{lm}(k)$ the lm component of the wavenumber dependent solute-dipole static correlation function, and $S_d^{lm}(k,t)$ the same component of the dipolar solvent dynamic structure factor. The latter, ($S_d^{lm}(k,t)$) provides an approximate description of the solvent's frictional response and consists of the rotational ($\Gamma_R(k,z)$) and translational ($\Gamma_T(k,z)$) memory kernels.[10] If one assumes diffusive relaxation for the isotropic dynamic structure factor, $\Gamma_T(k,z)$ can be obtained rather trivially from the centre-of-mass diffusion calculated using the medium viscosity and a suitable hydrodynamic boundary condition. However, one can include the inertial effects in the translational motion via a more accurate ion dynamic structure factor (see Eq. (13) of Ref. 18) but we have not done so as the subsequent calculations avoids direct inclusion of the inertial motions (both rotation and translation). Calculation of $\Gamma_R(k,z)$ is rather difficult and is usually obtained via the following connection to the experimental frequency dependent dielectric relaxation ($\varepsilon(z)$) in the collective limit:[86–89]

$$\frac{2k_BT}{I[z+\Gamma_R(k\sigma\rightarrow 0,z)]} = \frac{z\varepsilon_0[\varepsilon(z)-\varepsilon_\infty]}{f(110,k\sigma\rightarrow 0)\varepsilon_\infty[\varepsilon_0-\varepsilon(z)]}, \tag{21}$$

where ε_0 and ε_∞ are, respectively, the static and infinite frequency dielectric constants of the medium, I the moment of inertia of the rotating species. $f(110, k\sigma \rightarrow 0) = 1 - (\rho_d^0/4\pi)c(110, k\sigma \rightarrow 0)$.

It is clear from Eq. (21) that the experimental nature of $\varepsilon(z)$ (multi-exponential or stretched) will be transferred to the calculated polar solvation energy relaxation. This also means that any solvent dynamics, either pure rotational or collisional in character, which can impart a time-dependent change in the collective dipole moment autocorrelation function and thus contribute to $\varepsilon(z)$, will be included in the subsequent calculations of polar energy relaxation using Eq. (19). While the pure rotational contribution to $\varepsilon(z)$ falls in the microwave frequency regime (300 MHz–300 GHz),[90–93] the collisional or the translation-rotation coupling contribution emerges in the terahertz (1 THz = 10^3 GHz) range.[41,42] Dielectric relaxation measurements in the frequency range, $0.2 \leq \nu/\text{GHz} \leq 89$, of several of the RTILs studied here have reported $\varepsilon(z)$ in the following form:[23]

$$\varepsilon(z) = \varepsilon_\infty + \frac{S_1}{[1+(z\tau_1)^{1-\alpha_1}]^{\beta_1}} + \frac{S_2}{[1+z\tau_2]}, \tag{22}$$

with $\alpha_1 < 1$ and $\beta_1 = 1$ and τ_i being the relaxation time constant associated with the dispersion S_i. For [Bmim][BF_4] and [Bmim][PF_6] at ~298 K, τ_1 and τ_2 have been found to

be 284 ps and 620 fs, and 1178 ps, and 470 fs, with α_1 as 0.52 and 0.57, respectively. While the slower time constant (τ_1) has been ascribed to the exclusive reorientation of the cation dipole of these ILs, the faster one has been suspected to have contributions also from intermolecular vibration and other high frequency modes such as collision and translation-rotation coupling.[23] In what follows next, we use these two ILs as representative examples to show that ultrafast solvation timescale observed in DSS experiments can indeed arise in the present theory from the measured slowest dielectric relaxation step of these liquids in which ion translation or libration does not contribute at all.

Figure 7 depicts the decays of the predicted solvation response function due to solute-IL dipole-dipole interaction, $S_{sd}(t)$, for [Bmim][BF_4] and [Bmim][PF_6] at ~298 K in the limits of the collective ($k\sigma \rightarrow 0$) and the nearest neighbour ($k\sigma \rightarrow 2\pi$) modes of the orientational solvent polarization density fluctuation. These decays have been calculated by considering only the slowest step of the experimental dielectric relaxation[23] in Eq. (19) for the solute DCS.[18] Experimental results[2] are also shown in the same figure for a comparison. Parameters obtained from fits of these decays to a function, $S_{fit}(t) = a_1\exp(-t/\tau_1) + a_2\exp(-(t/\tau_2)^{\alpha})$, have also been shown in the insets. Analytical works described in the supplementary material (A1)[71] provide the necessary logic for

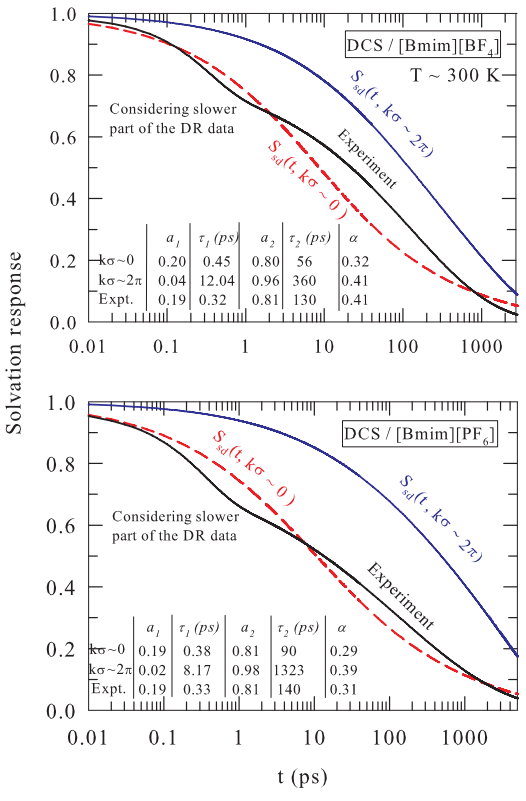

	a_1	τ_1 (ps)	a_2	τ_2 (ps)	α
kσ~0	0.20	0.45	0.80	56	0.32
kσ~2π	0.04	12.04	0.96	360	0.41
Expt.	0.19	0.32	0.81	130	0.41

	a_1	τ_1 (ps)	a_2	τ_2 (ps)	α
kσ~0	0.19	0.38	0.81	90	0.29
kσ~2π	0.02	8.17	0.98	1323	0.39
Expt.	0.19	0.33	0.81	140	0.31

FIG. 7. Comparison between the calculated dipole-dipole part of the solvation energy relaxation and the experimental response for DCS in [Bmim][BF_4] (upper panel) and [Bmim][PF_6] (lower panel) at ~300 K in the limits of the collective ($k\sigma \rightarrow 0$) and the nearest neighbour ($k\sigma \rightarrow 2\pi$) modes of the orientational solvent polarization density fluctuations. Note in calculations, only the slowest part of the experimental dielectric relaxation has been used as input.

suitability of the above fit function for the calculated solvation response functions in the $k\sigma \rightarrow 0$ and $k\sigma \rightarrow 2\pi$ limits even when one considers only the slowest but stretched component of the full experimental dielectric response. Both visual and numerical comparisons with experimental results strongly suggest that the pure reorientational dynamics of the dipolar cation can indeed generate an ultrafast polar solvation response in the collective limit with a time constant and amplitude very similar to those observed in the corresponding DSS experiments.[2] Interestingly, the calculated solvation response at $k\sigma \rightarrow 0$ limit also predicts the stretching exponent (α) very close and the slow time constant (τ_2) within a factor of 2 to those reported by the DSS experiments. The solvation response predicted at $k\sigma \rightarrow 2\pi$ limit is, on the other hand, is much slower and suggests overwhelming domination by the slow component (96%–98%) even-though the stretched exponential character of the dynamics has been reproduced qualitatively. The incorporation of the full experimental $\varepsilon(z)$[23] in the calculations leads to much faster decay of $S_{sd}(t)$ at the collective limit but brings the nearest neighbour response much closer to the experiments. This is shown in Fig. S4 of the supplementary material.[71] Interestingly, even with full $\varepsilon(z)$, the time constants associated with $S_{sd}(t)$ decays at $k\sigma \rightarrow 2\pi$ limit remain slower than those from experiments for these ILs, signifying the dominance of the collective polarization density fluctuation modes in the polar solvation energy relaxation in these coulomb fluids, particularly at short times. Interestingly, this is very similar to the predictions made earlier for polar solvation energy relaxation in conventional dipolar liquids.[10,94,95] This, however, does not suggest that the nearest neighbour solvent modes are unimportant. In fact, relaxations of both the orientational polarization density and isotropic ion density involving the nearest neighbour modes contribute to the slow long time decay so typical of these liquids.[17,18,21]

The closeness between the calculations at the collective limit and experiments observed in Fig. 7 then leads us to explore the relationship between the polar solvation response and the collective reorientational dynamics of dipolar IL species. This is along the line of what has been proposed earlier for short time dynamics in common dipolar solvents based on simulation results[85] and subsequently derived analytically in the limit of collective ($k\sigma \rightarrow 0$) dipolar solvent response.[86] Note the dipolar species is executing orientational relaxation in the force field of others and thus acquires a "collective" character in its single particle orientational motion.[29] For a strongly polar and homogeneous liquid where the polar solvation energy relaxation is much faster than the collective single particle orientation, the short time dynamics at the $k\sigma \rightarrow 0$ limit was predicted to be given by[86] $S_p(t) = [C_1(t)]^{\gamma} = [\exp(-t/\tau_I)^2]^{\gamma}$ where $\gamma = f(110, k\sigma \rightarrow 0) = \frac{3Y}{1-\varepsilon_0^{-1}}$ and $\tau_I = \sqrt{I/k_BT}$. The polarity parameter ($3Y$) is defined as[90] $3Y = \frac{4\pi\mu_{cation}^2\rho}{3k_BT}$, with μ_{cation} being the dipole moment of the dipolar species (cation here) and ρ the IL number density. Figure S5 (see supplementary material[71]) demonstrates that for [Bmim][BF_4], the relaxation of the polar solvation energy is much faster than that of the collective single particle orientational correlational function ($C_1(t)$) and thus fulfils one of the approximations made for strongly polar solvents. This is

a result representative of other imidazolium ILs as well and thus can be regarded as a general trend. The domination of the collective polarization mode in the early part of the polar solvation dynamics noticed in Fig. 7 for imidazolium ILs provides further support for carrying out the proposed analyses for these dipolar ILs. However, a direct comparison between the dipolar solvation response calculated from the present theory and that from $[\exp(-t/\tau_I)^2]^\gamma$ may not be proper for these ILs as inhomogeneity present in these liquids induces large departure of the cation reorientational dynamics from the isotropic rotational diffusion.[23,48,96,97] Anisotropic relaxation with large angle hopping motion[48] can give rise to fast energy relaxation in a way equivalent to that producing larger than the expected centre-of-mass diffusion in supercooled systems.[98–101] Even for these inhomogeneous liquids, we find that the calculated collective polar solvation response, $S_{sd}(t, k\sigma \to 0)$, can be mapped semi-quantitatively by the collective single particle orientational relaxation, $C_1(t)$, with a translation factor, γ. Note $C_1(t)$ is connected to $\varepsilon(z)$ via $\Gamma_R(k, z)$ as follows:[10] $C_1(t) = L^{-1}[z + \frac{2k_BT}{I\{z+\Gamma_R(k\sigma\to 0,z)\}}]^{-1}$, with Eq. (21) describing the relationship between $\varepsilon(z)$ and $\Gamma_R(k\sigma \to 0, z)$. Figure 8 presents such a depiction for DCS in [Bmim][BF_4], where only the slowest step of the experimental $\varepsilon(z)$ has been used for calculations. The near quantitative mapping of polar solvation response by the cation rotation at short times again strongly suggest that the solvent orientational polarization density relaxation can indeed generate the ultrafast response observed in DSS experiments. Note, however, that the value of the translation factor (γ) that has lead to the successful mapping of $S_{sd}(t)$ by $C_1(t)$ is approximately half of that (6.20) obtained from the relation, $\gamma = 3Y/(1-\varepsilon_0^{-1})$, using $\mu_{cation} \approx 3.7$ D.[102] If one uses $\mu_{cation} \approx 2.6$ D,[103] the value of γ turns out to be ~3, which is very close to the value (3.36) found here from mapping. This discrepancy, therefore, is more of a reflection of the non-uniqueness for the definition of the dipole moment of a charged species[104] than the inability of the cation rotational dynamics to describe the solvation energy relaxation in dipolar (here imidazolium) ILs. The comparison shown in Fig. 8 then do suggest that ultrafast polar solvation measured in DSS experiments with dipolar ILs can arise from the complex reorientational dynamics of the dipolar ions in these ILs.

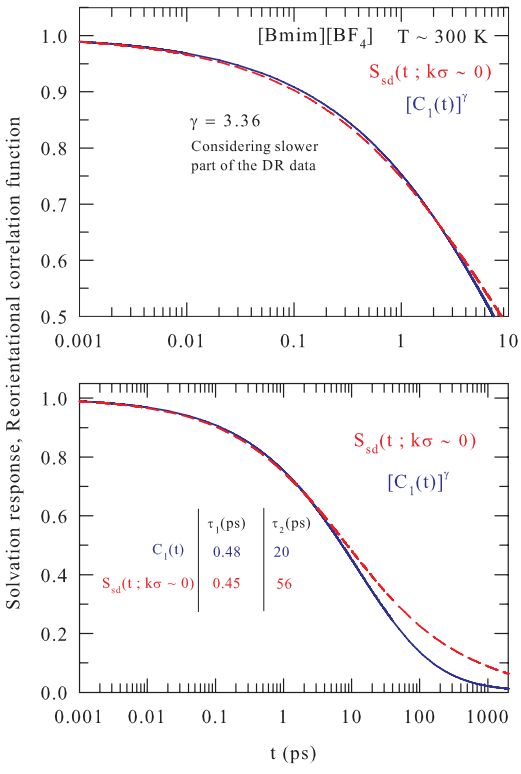

FIG. 8. Relation between the calculated polar solvation response, $S_{sd}(t)$, and the collective single particle reorientational correlation function, $C_1(t)$ for a dipolar IL, [Bmim][BF_4], at ~300 K. The calculations of $S_{sd}(t)$ are for the solute, DCS, at the limit of collective solvent polarization density fluctuations, and obtained by the slowest part of the experimental dielectric relaxation data. The upper panel shows the mapping of the solvation response by the single particle reorientational correlation function at short times and the lower panel at both short and long times.

IV. CONCLUSIONS

The work described here shows that the ultrafast solvation response in RTILs measured via 3PEPS experiments may have origin in the nearest neighbour solute-solvent non-dipolar interaction. When this non-dipolar interaction and that among solvent molecules are modelled as that given by the traditional LJ potential, the calculated fast time constants have been found to be in very good agreements with 3PEPS experiments for most of the RTILs. The calculated results also agree with the available simulation results and support the picture that sub-hundred femtosecond solvation response in ILs arises mainly from the nearest neighbour solute-IL interaction where solvent (or dipolar cation/anion) rotation plays an insignificant role. The regulatory nature of the nearest neighbour mode for nonpolar solvation energy relaxation forces the Debye-Huckel type description of spatial correlations inaccurate for explaining the 3PEPS and simulation results. A strong solute-solvent size ratio and density dependencies for the binary ultrafast solvation component have been predicted, which may be re-examined via suitable experiments. It is, however, to be mentioned here that electrostatic interaction can make the solvent structure around a dipolar solute more compact ("electrostriction"),[105,106] making the binary relaxation timescale much faster through the increased $g_{12}(\sigma)$ values.[107,108] Simulation studies of vibrational energy relaxation in ILs have already found the signature of it.[108] Such an enhancement of solvent density is not expected for a nonpolar solute and present calculations have also not considered this aspect (density enhancement) while predicting the rates for nonpolar solvation energy relaxation of a nonpolar solute in these ILs.

When the solute-IL dipolar solvation response is considered, it turns out to be the reorientational dynamics of the dipolar species (cation or anion), which can successfully describe the calculated polar solvation energy relaxation. Interestingly, the collective polar solvation response has been found to contain an ultrafast component, which is very close to that observed in the DSS experiments. The slowest component of the experimental dielectric relaxation data with its stretched exponential character alone is found to generate the ultrafast polar response in the imidazolium ILs in the limit of

the collective polarization density relaxation. The calculated dynamics presented here therefore suggest that the 3PEPS and DSS experiments measure the solvation response induced by the different components (non-dipolar and dipolar) of the total solute-IL interaction. However, it should be kept in mind that such a conclusion has been arrived after comparing the calculated dynamics to those from experiments that have used solutes of different characters--one (Ox4) that undergoes small dipole moment change upon excitation and the other (C153 or DCS) undergoes a large dipole moment change. So, the observed difference may partly arise from the difference in this solute character. Therefore, a comparison between the predicted results and those from 3PEPS and DSS measurements using the same solute is warranted for a more rigorous test of the above proposition. Applications of the present theory for a wider variety of ILs and comparison with experimental data (obtained using the same solute in 3PEPS and DSS measurements) should therefore be done in future.

ACKNOWLEDGMENTS

We thank Professor M. Maroncelli and Professor Y. Nagasawa for helpful comments. S.D. thanks the CSIR, India, for a research fellowship.

[1] M. Muramatsu, Y. Nagasawa, and H. Miyasaka, J. Phys. Chem. A **115**, 3886 (2011).
[2] S. Arzhantsev, H. Jin, G. A. Baker, and M. Maroncelli, J. Phys. Chem. B **111**, 4978 (2007).
[3] N. Ito, S. Arzhantsev, M. Heitz, and M. Maroncelli, J. Phys. Chem. B **108**, 5771 (2004).
[4] C. J. Bardeen, S. J. Rosenthal, and C. V. Shank, J. Phys. Chem. A **103**, 10506 (1999).
[5] G. Blanchard, Chem. Phys. **138**, 365 (1989).
[6] M. Maroncelli and G. R. Fleming, J. Chem. Phys. **89**, 5044 (1988).
[7] E. A. Carter and J. T. Hynes, J. Chem. Phys. **94**, 5961 (1991).
[8] C. P. Hsu, X. Song, and R. A. Marcus, J. Phys. Chem. B **101**, 2546 (1997).
[9] X. Song and D. Chandler, J. Chem. Phys. **108**, 2594 (1998).
[10] B. Bagchi and R. Biswas, Adv. Chem. Phys. **109**, 207 (1999).
[11] A. Samanta, J. Phys. Chem. B **110**, 13704 (2006).
[12] H. Jin, G. A. Baker, S. Arzhantsev, J. Dong, and M. Maroncelli, J. Phys. Chem. B **111**, 7291 (2007).
[13] P. K. Chowdhury, M. Halder, L. Sanders, T. Calhoun, J. L. Anderson, D. W. Armstrong, X. Song, and J. W. Petrich, J. Phys. Chem. B **108**, 10245 (2004).
[14] B. Lang, G. Angulo, and E. Vauthey, J. Phys. Chem. A **110**, 7028 (2006).
[15] J. A. Ingram, R. S. Moog, N. Ito, R. Biswas, and M. Maroncelli, J. Phys. Chem. B. **107**, 5926 (2003).
[16] H. K. Kashyap and R. Biswas, J. Phys. Chem. B **112**, 12431 (2008).
[17] H. K. Kashyap and R. Biswas, J. Phys. Chem. B **114**, 16811 (2010).
[18] H. K. Kashyap and R. Biswas, J. Phys. Chem. B **114**, 254 (2010).
[19] H. K. Kashyap and R. Biswas, Indian J. Chem. A **49**, 685 (2010).
[20] S. Daschakraborty and R. Biswas, J. Phys. Chem. B **115**, 4011 (2011).
[21] S. Daschakraborty and R. Biswas, Chem. Phys. Lett. **510**, 210 (2011); **545**, 54 (2012).
[22] A. Stoppa, J. Hunger, R. Buchner, G. Hefter, A. Thoman, and H. Helm, J. Phys. Chem. B **112**, 4854 (2008).
[23] J. Hunger, A. Stoppa, S. Schrodle, G. Hefter, and R. Buchner, Chem. Phys. Chem. **10**, 723 (2009).
[24] M.-M. Huang, S. Bulut, I. Crossing, and H. Weingertner, J. Chem. Phys. **133**, 101101 (2010).
[25] O. Zech, J. Hunger, J. R. Sangoro, C. Iacob, F. Cremer, W. Kunz, and R. Buchner, Phys. Chem. Chem. Phys. **12**, 14341 (2010).
[26] T. Joo, Y. Jia, J.-Y. Yu, M. J. Lang, and G. R. Fleming, J. Chem. Phys. **104**, 6089 (1996).
[27] M. L. Horng, J. A. Gardecki, A. Papazyan, and M. Maroncelli, J. Phys. Chem. **99**, 17311 (1995).
[28] D. Bingemann and N. P. Ernsting, J. Chem. Phys. **102**, 2691 (1995).
[29] R. Biswas, N. Nandi, and B. Bagchi, J. Phys. Chem. B **101**, 2968 (1997).
[30] S. Mukamel, Annu. Rev. Phys. Chem. **41**, 647 (1990).
[31] Y. J. Yan and S. Mukamel, J. Chem. Phys. **94**, 179 (1991).
[32] L. Reynolds, J. A. Gardecki, S. J. V. Frankland, M. L. Horng, and M. Maroncelli, J. Phys. Chem. **100**, 10337 (1996).
[33] J. Ma, D. V. Bout, and M. Berg, J. Chem. Phys. **103**, 9146 (1995).
[34] J. T. Fourkas, A. Benigno, and M. Berg, J. Chem. Phys. **99**, 8552 (1993).
[35] J. T. Fourkas and M. Berg, J. Chem. Phys. **98**, 7773 (1993).
[36] J. P. Hansen and I. R. McDonald, *Theory of Simple Liquids*, 3rd ed. (Academic, San Diego, 2006).
[37] U. Balucani and M. Zoppi, *Dynamics of the Liquid State* (Clarendon, Oxoford, 1994).
[38] B. Bagchi and S. Bhattacharyya, Adv. Chem. Phys. **116**, 67 (2007).
[39] R. Biswas, S. Bhattacharyya, and B. Bagchi, J. Chem. Phys. **108**, 4963 (1998).
[40] B. Bagchi, J. Chem. Phys. **100**, 6658 (1994).
[41] C. Schroder, J. Hunger, A. Stoppa, R. Buchner, and O. Steinhauser, J. Chem. Phys. **129**, 184501 (2008).
[42] C. Schroder, M. Haberler, and O. Steinhauser, J. Chem. Phys. **128**, 134501 (2008).
[43] D. A. Turton, J. Hunger, A. Stoppa, G. Hefter, A. Thoman, M. Walther, R. Buchner, and K. Wynne, J. Am. Chem. Soc. **131**, 11140 (2009).
[44] D. Roy and M. Maroncelli, J. Phys. Chem. B **116**, 5951 (2012).
[45] D. Jeong, Y. Shim, M. Y. Choi, and H. J. Kim, J. Phys. Chem. B **111**, 4920 (2007).
[46] Y. Shim, M. Y. Choi, and H. J. Kim, J. Chem. Phys. **122**, 044511 (2005).
[47] Y. Shim, J. Duan, M. Y. Choi, and H. J. Kim, J. Chem. Phys. **119**, 6411 (2003).
[48] Y. Shim and H. J. Kim, J. Phys. Chem. B **112**, 11028 (2008).
[49] Y. Shim and H. J. Kim, J. Phys. Chem. B **113**, 12964 (2009).
[50] Y. Shim and H. J. Kim, J. Phys. Chem. B **111**, 4510 (2007).
[51] Y. Shim, D. Jeong, M. Y. Choi, and H. J. Kim, J. Chem. Phys. **125**, 061102 (2006).
[52] I. Streeter, R. M. Lynden-Bell, and R. G. Compton, J. Phys. Chem. C **112** 14538 (2008).
[53] B. L. Bhargava and S. Balasubramanian, J. Chem. Phys. **123**, 144505 (2005).
[54] M. N. Kobrak and V. Znamenskiy, Chem. Phys. Lett. **395**, 127 (2004).
[55] M. N. Kobrak, J. Chem. Phys. **125**, 064502 (2006).
[56] M. N. Kobrak, J. Chem. Phys. **127**, 184507 (2007).
[57] M. N. Kobrak, J. Chem. Phys. **127**, 099903 (2007).
[58] M. D. Stephens, J. G. Saven, and J. L. Skinner, J. Chem. Phys. **106**, 2129 (1997).
[59] J. D. Weeks, D. Chandler, and H. C. Andersen, J. Chem. Phys. **54**, 5237 (1971).
[60] S. Chandrasekhar, Rev. Mod. Phys. **15**, 1 (1943).
[61] H. Stehfest, Commun. ACM **13**, 624 (1970).
[62] J. L. Lebowitz, Phys. Rev. **133**, A895 (1964).
[63] K. Hoshino, J. Phys. F: Met. Phys. **13**, 1981 (1983)
[64] R. V. G. Rao and A. Satpathy, Phys. Rev. B **41**, 11938 (1990)
[65] P. Attard, Phys. Rev. E **48**, 3604 (1993).
[66] A. Chandra and B. Bagchi, J. Chem. Phys. **110**, 10024 (1999).
[67] S. Glasstone, *An Introduction to Electrochemistry* (Litton Educational Publishing, New York, 1942).
[68] C. F. Chapman and M. Maroncelli, J. Phys. Chem. **95**, 9095 (1991).
[69] C. Daguenet, P. J. Dyson, I. Krossing, A. Oleinikova, J. Slattery, C. Wakai, and H. Weingärtner, J. Phys. Chem. B **110**, 12682 (2007).
[70] J. G. Huddleston, A. E. Visser, W. M. Reichert, H. D. Willauer, G. A. Broker, and R. D. Rogers, Green Chem. **3**, 156 (2001).
[71] See supplementary material at http://dx.doi.org/10.1063/1.4752425 for information regarding solute-RTIL size ratio, RTIL densities, ion diameters, density dependence of radial distribution function at contact and structural relaxation, calculated solvation response functions for [Bmim][BF_4] and [Bmim][PF_6] at the collective and nearest neighbor limits, decay of orientational correlation function and polar solvation response function, and the derivation of how one arrives at a bi-modal solvation response using only the slowest (but stretched) part of the full experimental dielectric relaxation data.
[72] K. Fuji, T. Fujimori, T. Takamuku, R. Kanzaki, Y. Umebayashi, and S. Ishiguro, J. Phys. Chem. B **110**, 8179 (2006).
[73] C. S. Santos, H. V. R. Annapureddy, N. S. Murthy, H. K. Kashyap, E. W. Castner, Jr., and C. Margulis, J. Chem. Phys. **134**, 064501 (2011).

[74]G.-E. Logotheti, J. Ramos, and I. C. Economou, J. Phys. Chem. B **113**, 7211 (2009).
[75]A. Triolo, O. Russina, B. Fazio, G. B. Appetecchi, M. Carewska, and S. Passerini, J. Chem. Phys. **130**, 164521 (2009).
[76]A. Triolo, O. Russina, B. Fazio, R. Triolo, and E. D. Cola, Chem. Phys. Lett. **467**, 362 (2008).
[77]P. K. Mandal, M. Sarkar, and A. Samanta, J. Phys. Chem. A **108**, 9048 (2004).
[78]Y. Wang and G. A. Voth, J. Am. Chem. Soc. **127**, 12192 (2005).
[79]Z. Hu and C. J. Margulis, Proc. Natl. Acad. Sci. U.S.A. **103**, 831 (2006).
[80]A. Adhikari, A. K. Sahu, S. Dey, S. Ghosh, U. Mandal, and K. Bhattacharyya, J. Phys. Chem. B **111**, 12809 (2007).
[81]H. Jin, X. Li, and M. Maroncelli, J. Phys. Chem. B **111**, 13473 (2007).
[82]D. K. Sasmal, A. K. Mandal, T. Mondal, and K. Bhattacharyya, J. Phys. Chem. B **115**, 7781 (2011).
[83]A. Samanta, J. Phys. Chem. Lett. **1**, 1557 (2010).
[84]M. Maroncelli, X.-X. Zhang, M. Liang, D. Roy, and N. P. Ernsting, Faraday Discuss. Chem. Soc. **154**, 409 (2012).
[85]M. Maroncelli, V. P. Kumar, and A. Papazyan, J. Phys. Chem. **97**, 13 (1993).
[86]S. Roy and B. Bagchi, Chem. Phys. **183**, 207 (1994).
[87]S. Roy and B. Bagchi, J. Chem. Phys. **99**, 9938 (1993).
[88]S. Roy and B. Bagchi, J. Chem. Phys. **99**, 1310 (1993).
[89]N. Nandi, S. Roy, and B. Bagchi, J. Chem. Phys. **102**, 1390 (1995).
[90]C. G. Gray and K. E. Gubbins, *Theory of Molecular Fluids* (Clarendon, Oxford, UK, 1984), Vol. I.
[91]X. Song, J. Chem. Phys. **131**, 044503 (2009).
[92]C. Schroder, M. Haberler, and O. Steinhauser, J. Chem. Phys. **131**, 114504 (2009).
[93]C. Schroder, C. Wakai, H. Weingartner, and O. Steinhauser, J. Chem. Phys. **136**, 084511 (2007).
[94]B. Bagchi and A. Chandra, Adv. Chem. Phys. **80**, 1 (1991).
[95]B. Bagchi and A. Chandra, J. Chem. Phys. **97**, 5126 (1992).
[96]N. E. Heimer, J. S. Wilkes, P. C. Wahlbeck, and W. R. Carper, J. Phys. Chem. A **110**, 868 (2006).
[97]T. Koddermann, R. Ludwig, and D. Paschek, Chem. Phys. Chem. **9**, 1851 (2008).
[98]J. Habasaki and K. L. Ngai, J. Chem. Phys. **129**, 194501 (2008).
[99]T. Pal and R. Biswas, Chem. Phys. Lett. **517**, 180 (2011).
[100]B. Guchhait, S. Daschakraborty, and R. Biswas, J. Chem. Phys. **136**, 174503 (2012).
[101]B. Guchhait, H. A. R. Gazi, H. K. Kashyap, and R. Biswas, J. Phys. Chem. **114**, 5066 (2010).
[102]H. Jin, B. O'Hare, J. Dong, S. Arzhantsev, G. A. Baker, J. F. Wishart, A. J. Benesi, and M. Maroncelli, J. Phys. Chem. B **112**, 81 (2008).
[103]B. L. Bhargava and S. Balasubramanian, J. Phys. Chem. B **111**, 4477 (2007).
[104]M. N. Kobrak and N. Sandalow, *Molten Salts XIV*, edited by A. Mantz and P. Trulove (Electrochemical Society, Pennington, NJ, 2006).
[105]A. Papazyan and M. Maroncelli, J. Chem. Phys. **102**, 2888 (1995).
[106]P. V. Kumar and M. Maroncelli, J. Chem. Phys. **112**, 5370 (2000).
[107]S. Daschakraborty and R. Biswas, J. Chem. Sci. **124**, 763 (2012).
[108]Y. Shim and H. J. Kim, J. Chem. Phys. **125**, 024507 (2006).